

# Interannual Heat Content Variability and Lagrangian Pathways in the Tropical Pacific

Christina L. Holland and Gary T. Mitchum,

College of Marine Science, USF, 140 Seventh Avenue South, St. Petersburg, FL 33701  
 cholland@marine.usf.edu  
 mitchum@marine.usf.edu

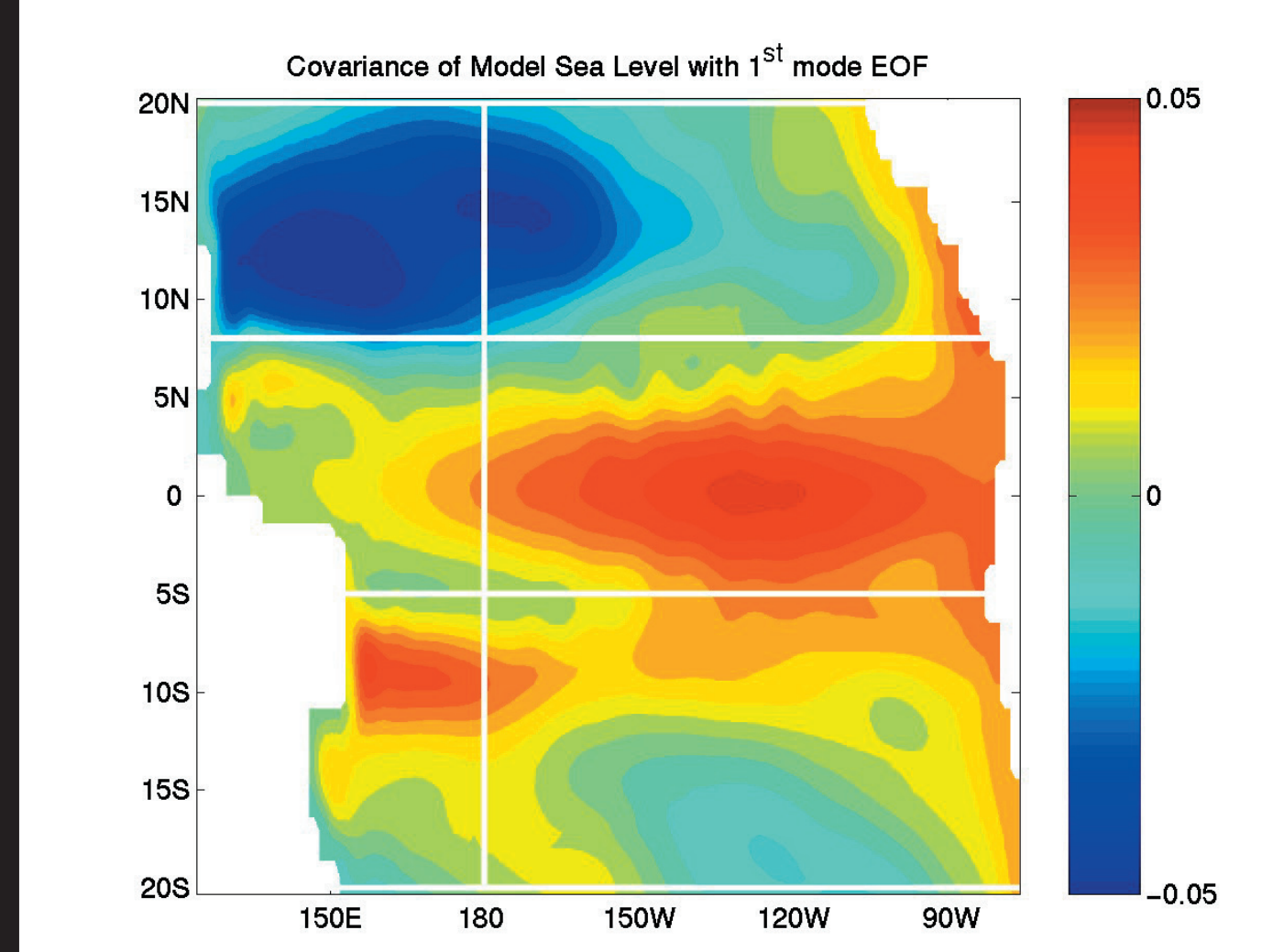
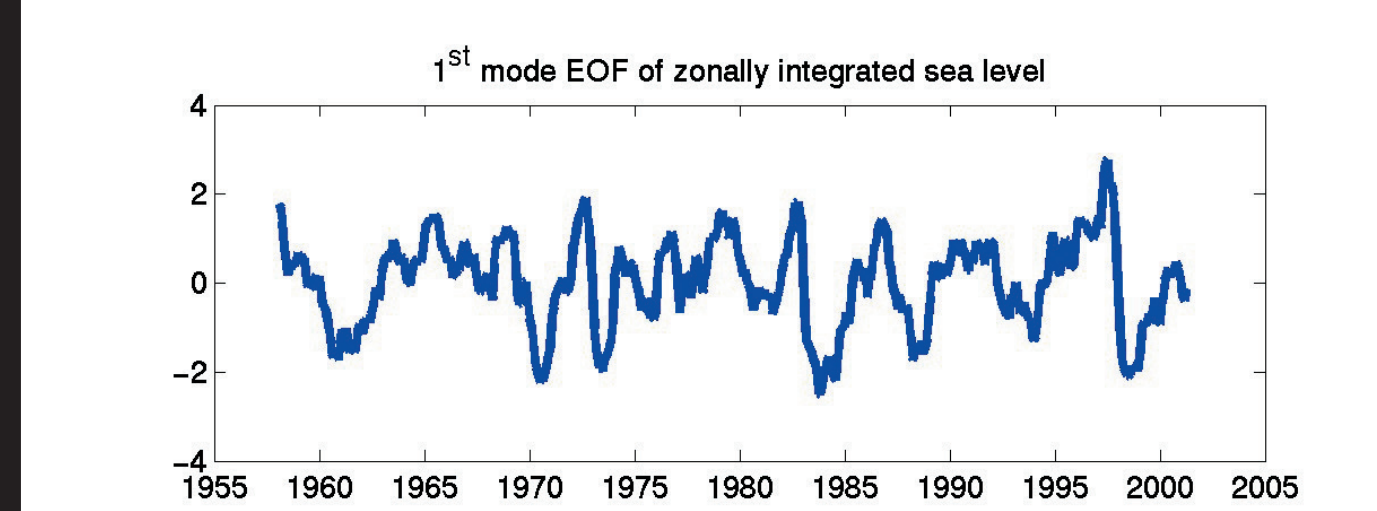
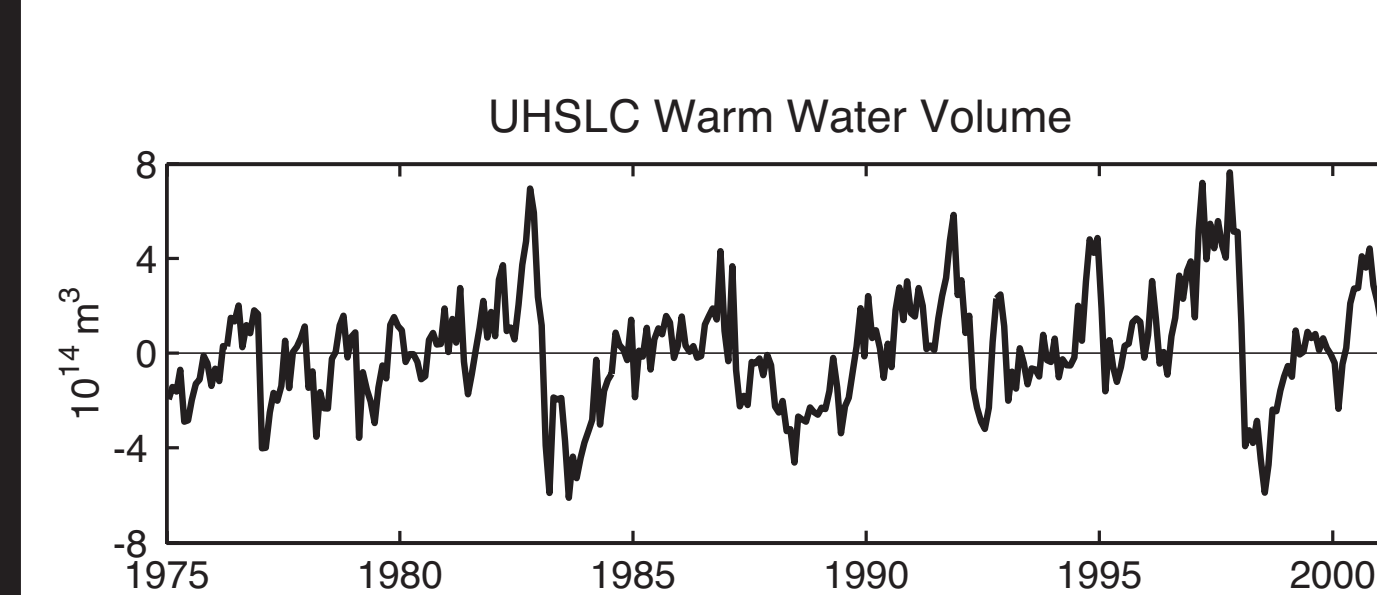


## Abstract

At previous SWT meetings, we have presented results describing the large-scale two-dimensional patterns of volume variability in the tropical Pacific during the El Niño – Southern Oscillation (ENSO) cycle. We determined that the volume variability could be accounted for by the variations in the vertically integrated heat content. As a result, we then looked in greater detail at the transport pathways in the tropical Pacific that gave rise to heat content anomalies during ENSO. We did this by computing Lagrangian trajectories backwards in time from several anomaly regions, and our computations were based on the output of a modified version of the Gent and Cane (1989) sigma-coordinate model. These results will be briefly reviewed. Based on feedback from previous SWT meetings, we have continued by examining whether our results are robust. First, we computed trajectories for a Gaussian clump of initial positions, to see whether the trajectories would remain coherent as we tracked them back through time. Next, we completed two test runs of the model, in which the mixed layer dynamics were altered to allow for greater and lesser degrees of wind stirring, and another run wherein the mixed layer depth was fixed at fifty meters. The trajectory calculations and analysis were repeated for each of these runs for the eastern equatorial warm anomaly and for the off-equatorial cool anomalies in the western Pacific. Finally, we are completing an additional model run with daily output, in order to check whether the trajectories computed from monthly averaged output of the model are consistent with trajectories computed from fields with finer temporal resolution.

## Review of Previous Results

We began by describing the horizontal patterns of volume change and redistribution within the tropical Pacific. The question of whether or not the volume of the tropical Pacific changes over the course of an El Niño event has important consequences for our understanding of the dynamical mechanisms responsible for the variability. Computations of volume variability based on the tide gauge network within the tropical Pacific, shown in the figure on the top left, suggests that the tropical Pacific as a whole build up volume prior to warm ENSO events, and experiences a rapid loss during the event itself.

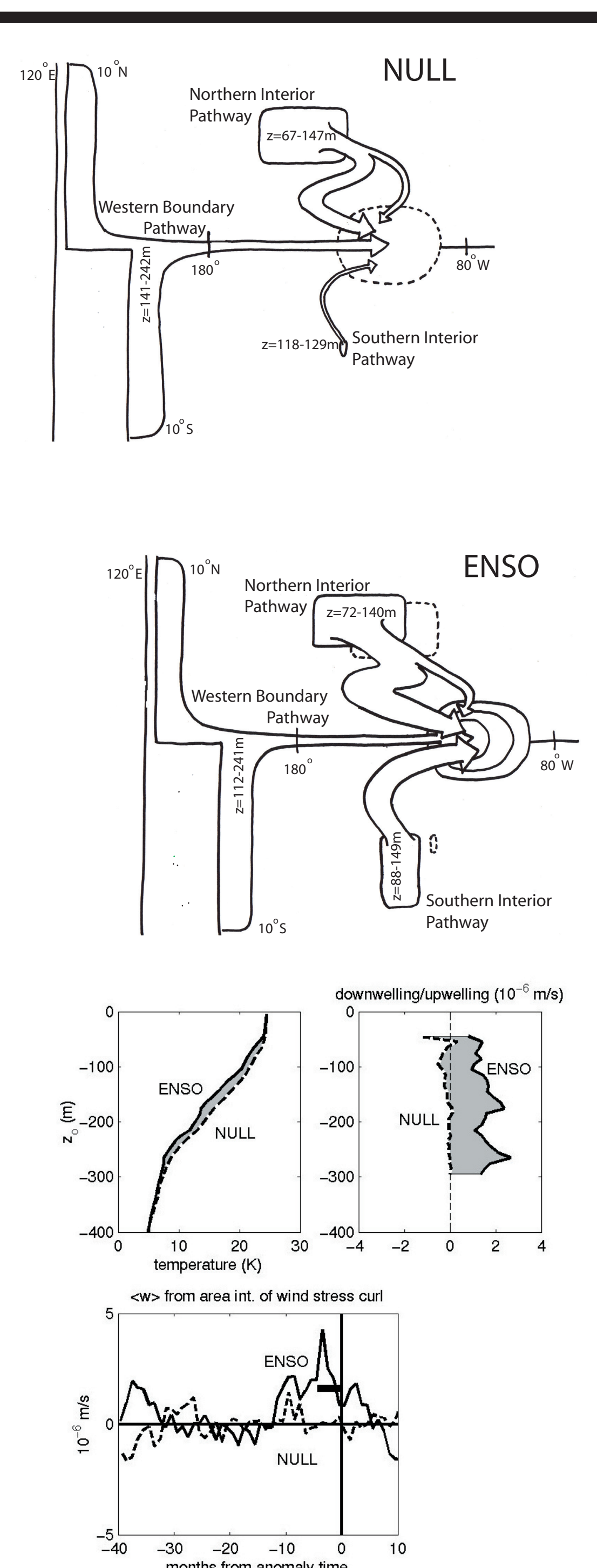


Revisiting this question using TOPEX / Poseidon (T/P) altimetry and a numerical model based on Gent and Cane (1989), we found that the tide gauge volume estimate is more accurately a description of the volume variability over approximately 6°S–6°N. T/P altimetry and our numerical model results show that the near-equatorial volume is largely countered by a volume increase between 8°N and 20°N, but that there is still a decrease over the tropical Pacific as a whole. Using the numerical model fields, we described the pattern of volume redistribution in the tropical Pacific by computing the dynamics responsible for volume variability in a series of geographic boxes and the fluxes between each. These boxes are shown in the figure below left, superimposed over a map of the covariance of sea surface height with the primary mode of variability of the zonally averaged sea surface height (thus capturing the meridional redistribution). The fluxes responsible for the redistribution between these boxes is shown in schematic form in the figure below. The major terms are the near equatorial eastward heat flux, the redistribution to the south of the equator, the northward heat flux across 8°N, and the upward surface heat flux in the eastern equatorial region. All these contribute to a net loss in the equatorial and southern boxes over an ENSO event, and a corresponding gain in the northern boxes. The net fluxes out of the tropics are relatively small. The volume variability within the tropical Pacific, or within any of our smaller geographic boxes, can be accounted for almost entirely by changes in the vertically integrated heat content.

More recently, we have focused on the heat content anomalies throughout ENSO. Using model temperature and velocity fields, we have computed trajectories backward in time from locations within strong ENSO heat content anomalies. By comparing trajectories computed during ENSO conditions to trajectories computed during normal (NULL) conditions, we can compute diagnostic terms for each water parcel. These are: the initial anomaly (we chose the length of the trajectory so that this term is small), the zonal, meridional, and vertical effects of the temperature gradient between the ENSO and NULL initial positions, the difference in surface heating during ENSO and NULL conditions, and the difference in (NULL) surface heating experience by the water parcel due to differences between the ENSO and NULL pathways.

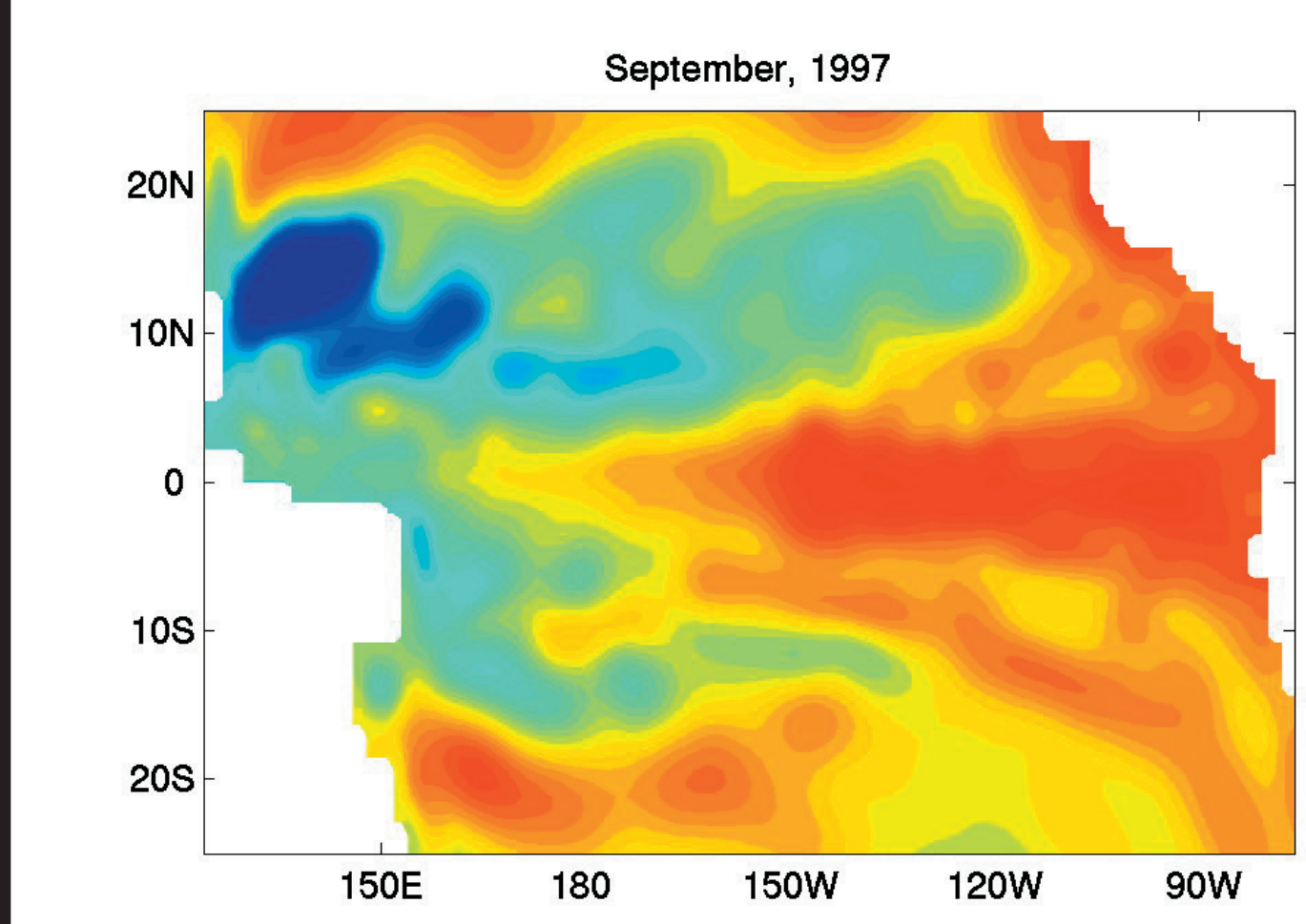
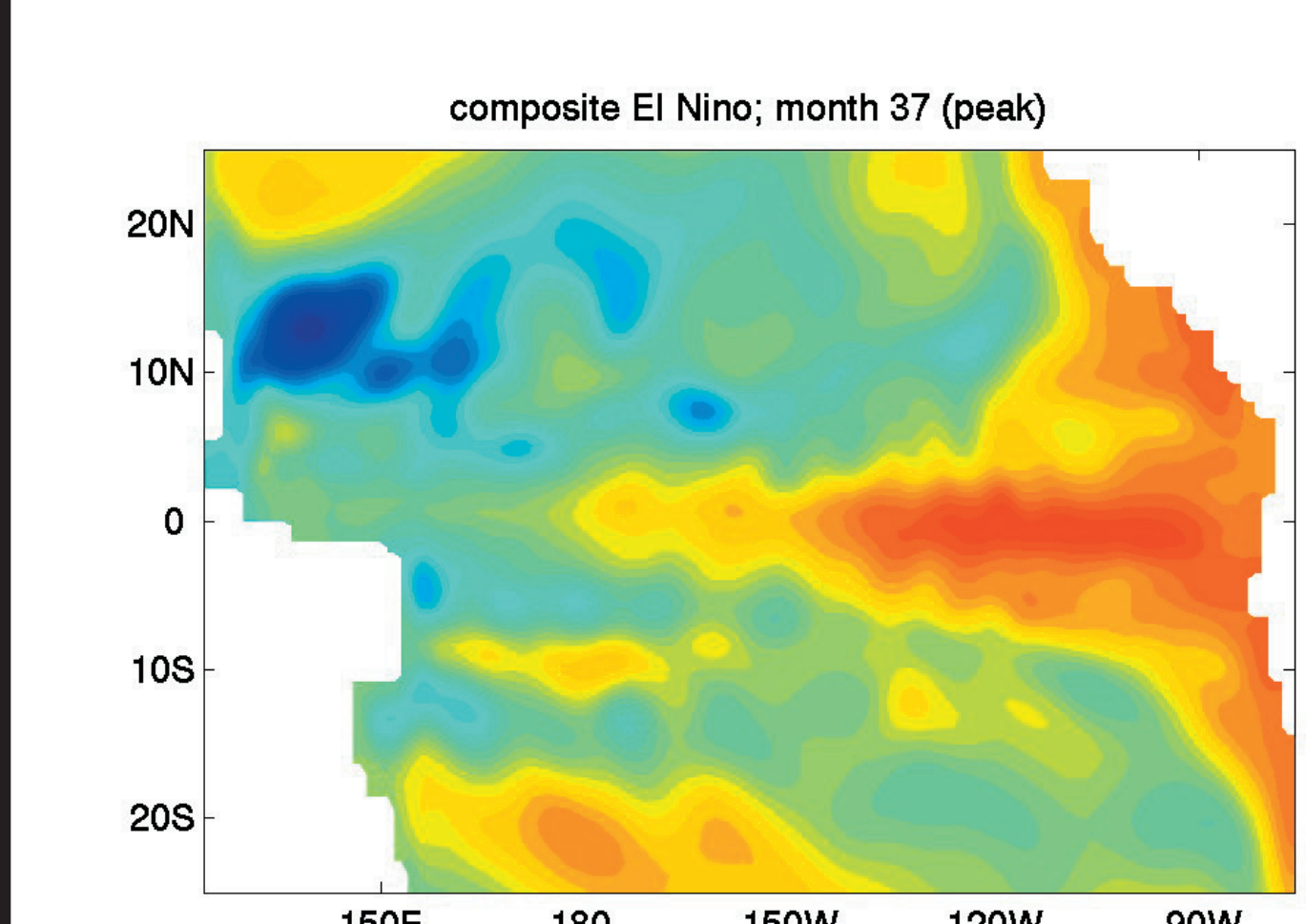
For example, we determined that there are three main pathways into the eastern equatorial Pacific, a western boundary pathway and two interior pathways, from north and south of the equator, shown schematically in the figure on the top right. During ENSO, all three pathways are shallower in origin, and the two interior pathways are much stronger and their origins are further west. These factors combine to create the familiar strong warm anomaly in the eastern equatorial Pacific at the peak of the El Niño event.

We also diagnosed off-equatorial warm anomalies in both the eastern Pacific (warm anomalies) and the western Pacific (cool anomalies) a few months after the peak of El Niño. The cool anomalies in the western off-equatorial Pacific were especially interesting. They are due to increased upwelling during El Niño, and they can be accounted for by changes in the local wind stress curl and Ekman pumping in the region, as shown at right.



## Our Composite Compared to the 1997 ENSO Event

In the analyses described above, we used a composite ENSO event, which was formed by averaging 4 distinct ENSO periods. Specifically, these are the 1972–1973, 1982–1983, 1986–1987, and 1997–1998 ENSO events. We did this to describe the progression of volume changes and redistribution within a typical ENSO event. Of course, there is considerable variation in the details from one event to another, but that is beyond the scope of the current study.



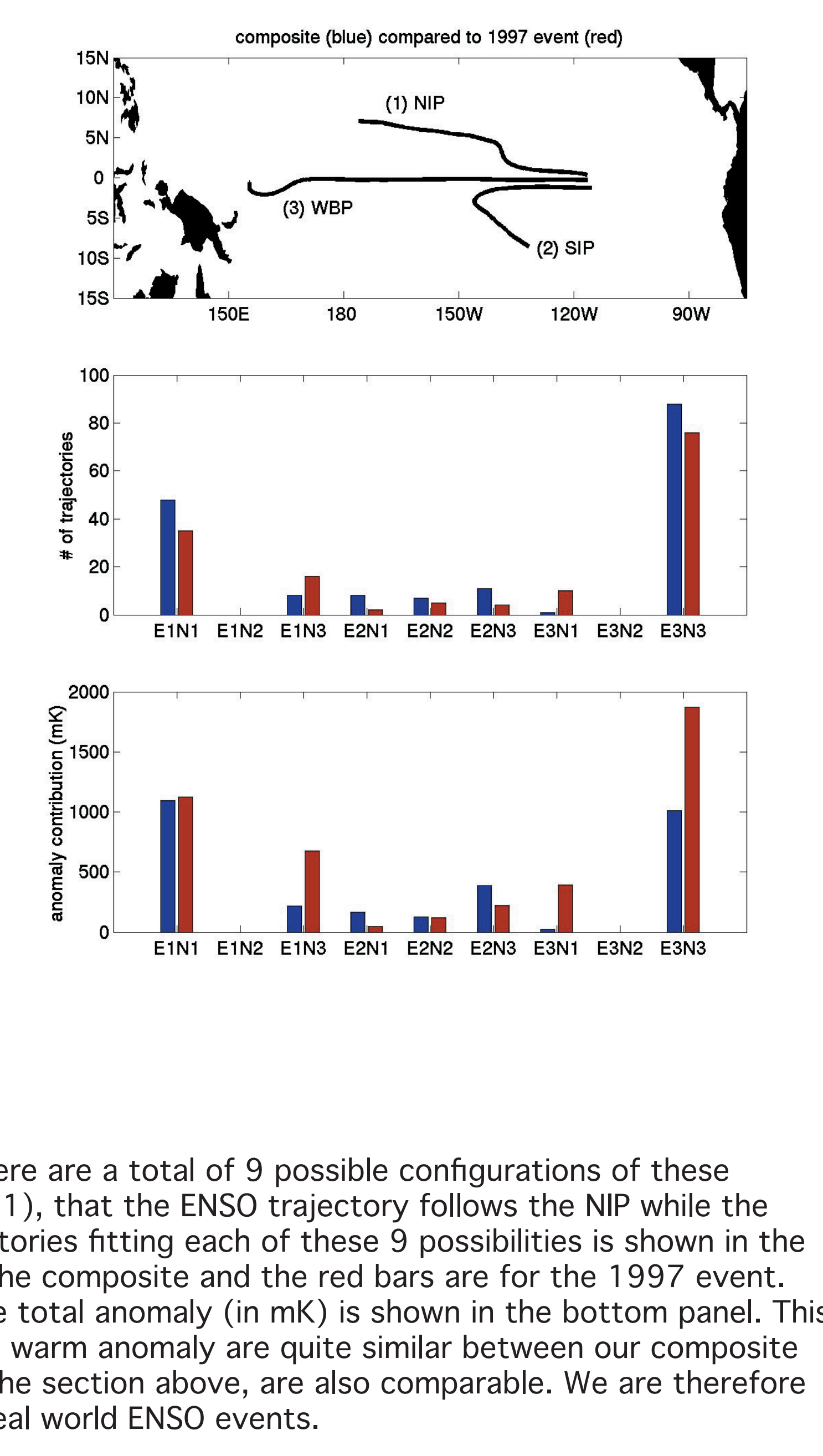
We decided to check the composite ENSO by repeating the analysis of the eastern equatorial warm anomaly using just the 1997 ENSO event, and comparing that to the results from the composite ENSO. The composite was formed by averaging the four events listed above, with no normalization. Since the 1997 event was such an extremely strong event, we expected that the composite would be similar in character to this one particular event.

In fact, the composite and the 1997 ENSO events are qualitatively similar, although the 1997 event is the stronger of the two. The figure on the left shows maps of the vertically integrated heat content anomaly for these two events. The top panel shows the eastern equatorial warm anomaly at month 37, the peak of the composite ENSO event. This month corresponds to September of 1997, which is shown in the lower panel.

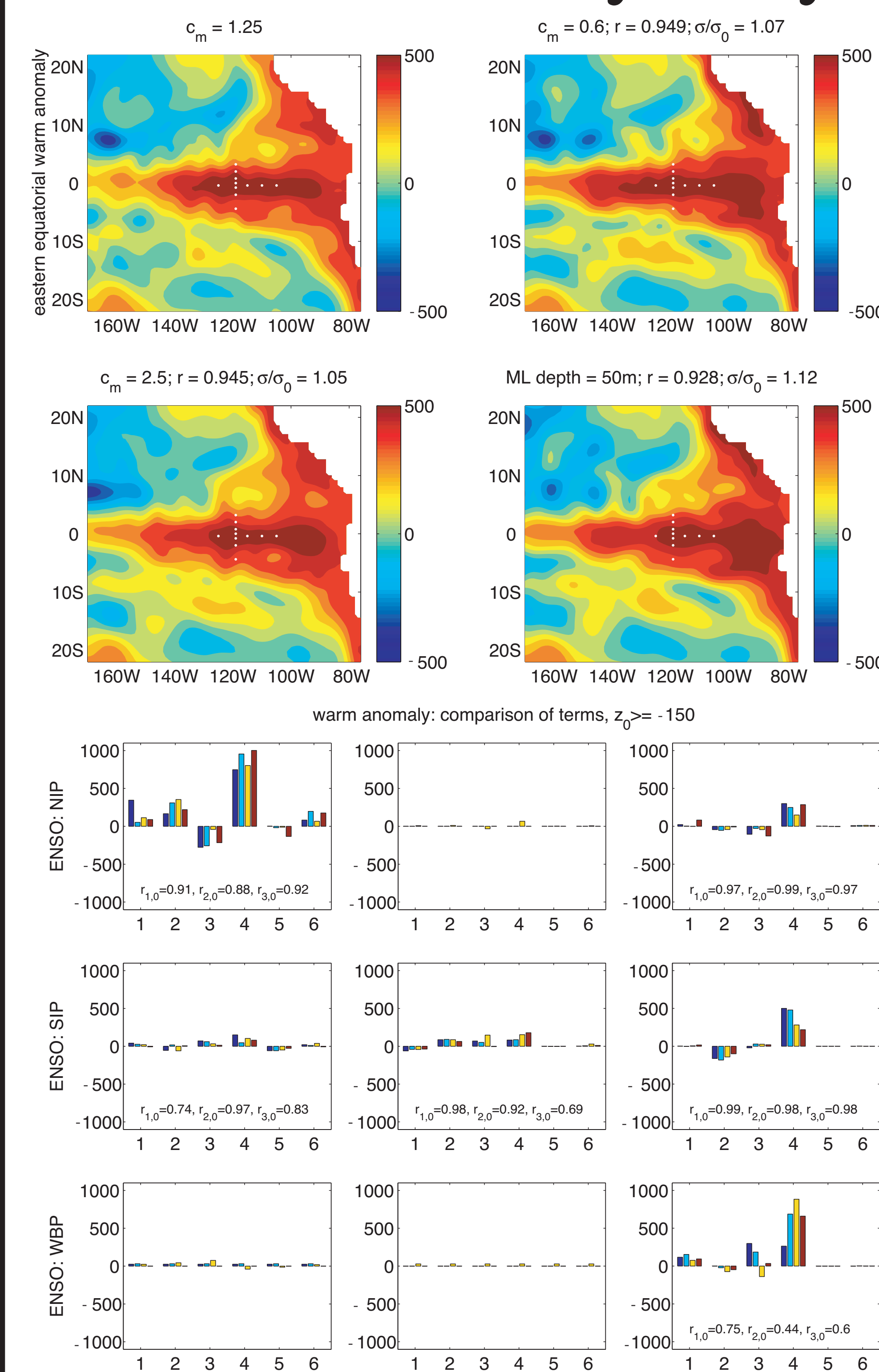
The figure below shows the vertical profile of the temperature anomaly for this month, averaged horizontally over the anomaly region. Again, they are qualitatively similar, but the 1997 event (shown in green) has a temperature anomaly that is approximately 50% greater than the temperature anomaly for the composite event (shown in blue). Also, the temperature anomaly at depth (near 200m) is proportionately higher in the 1997 event than in the composite. This suggests that there are dynamical differences between the 1997 event and the other ENSO events used to form the composite, but the anomaly in this depth range is small when compared to the anomaly near the surface.

Trajectories were computed as well for the 1997 event, starting from the same positions as were used with the composite. As with the composite, the trajectories entering the anomaly region in the upper 150m (accounting for most of the anomaly) followed three major pathways: the Northern Interior Pathway (1, NIP), the Southern Interior Pathway (2, SIP), and the Western Boundary Pathway (3, WBP), shown schematically in the top panel of the figure above and to the right.

Since trajectories were computed for both ENSO and NULL cases, there are a total of 9 possible configurations of these pathways: that the ENSO and NULL trajectories both follow the NIP (E1N1), that the ENSO trajectory follows the NIP while the NULL trajectory follows the SIP (E1N2), and so on. The number of trajectories fitting each of these 9 possibilities is shown in the middle panel of the figure above and to the right. The blue bars are for the composite and the red bars are for the 1997 event. Similarly, the amount that each of these 9 possible scenarios adds to the total anomaly (in mK) is shown in the bottom panel. This figure shows that the dynamics which give rise to the western equatorial warm anomaly are quite similar between our composite ENSO and the 1997 warm event. The diagnostic terms, as discussed in the section above, are also comparable. We are therefore confident that our composite is yielding results which are applicable to real world ENSO events.



## Model Mixed Layer Dynamics

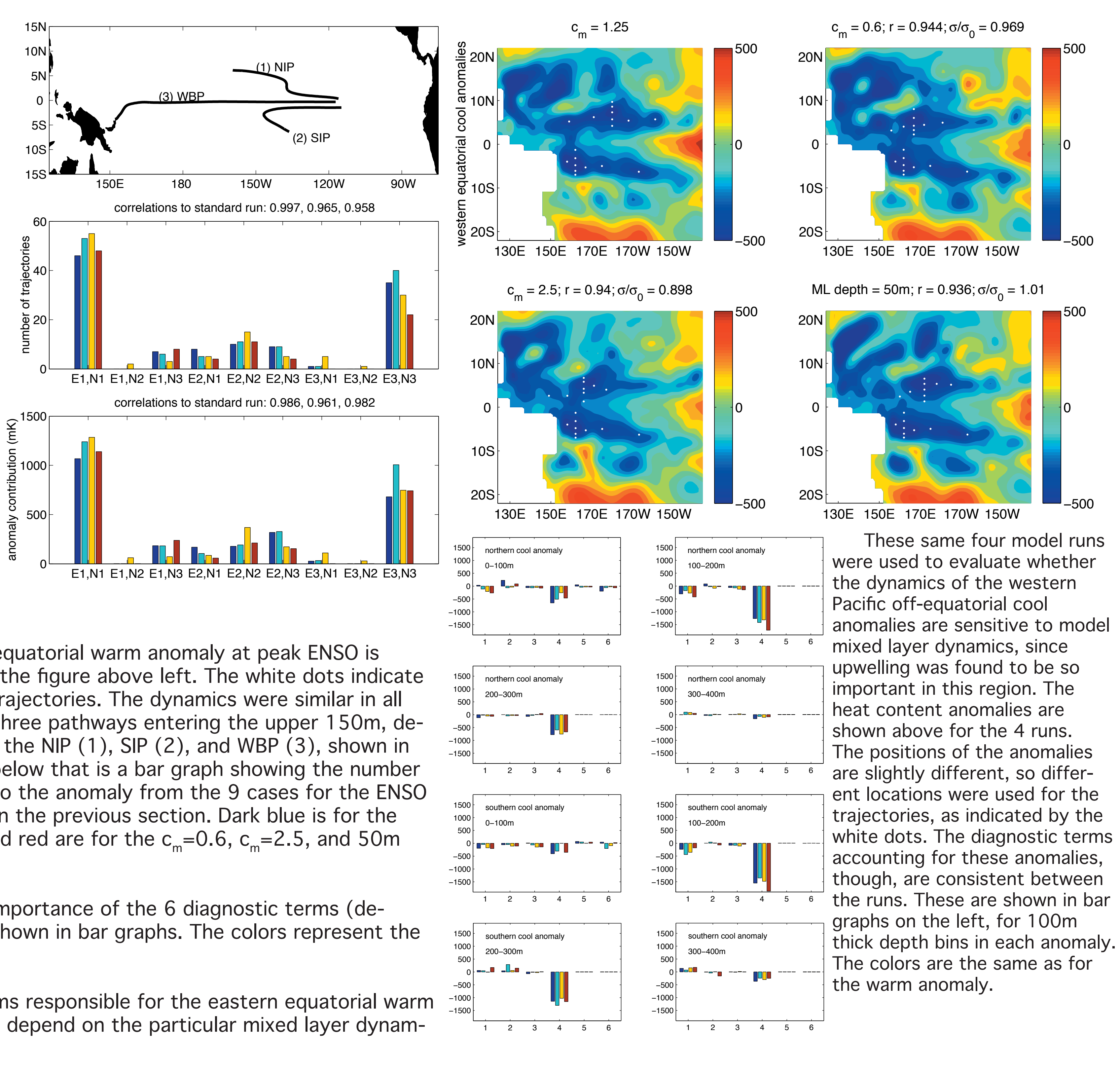


Since so much of the heat content and volume variability of the tropical Pacific is due to ENSO-related changes in the vertical movement of water parcels, the dynamics of the mixed layer are clearly important. This model uses a hybrid vertical mixing scheme (Chen et al., 1994), which includes the effects of wind stirring, shear instability, and convective overturning. This scheme includes a tunable parameter controlling the degree of wind stirring. In the base model run, this parameter is set to  $c_m=1.25$ . We have completed two additional runs, with this parameter set to  $c_m=0.6$  and  $c_m=2.5$ . One other run was completed, in which the mixed layer was simply held at 50m thick, everywhere. The horizontal patterns of volume variability and redistribution were similar for all of these model runs.

The heat content in the eastern equatorial warm anomaly at peak ENSO is shown, for these four model runs, in the figure above left. The white dots indicate the spatial points used to compute trajectories. The dynamics were similar in all cases. The anomaly arises from the three pathways entering the upper 150m, described in the review section above: the NIP (1), SIP (2), and WBP (3), shown in the figure above right. Immediately below that is a bar graph showing the number of trajectories and the contribution to the anomaly from the 9 cases for the ENSO and NULL trajectories, as described in the previous section. Dark blue is for the control run, and light blue, yellow, and red are for the  $c_m=0.6$ ,  $c_m=2.5$ , and 50m mixed layer runs.

In the figure at left, the relative importance of the 6 diagnostic terms (described above) for these 9 cases is shown in bar graphs. The colors represent the different runs, as before.

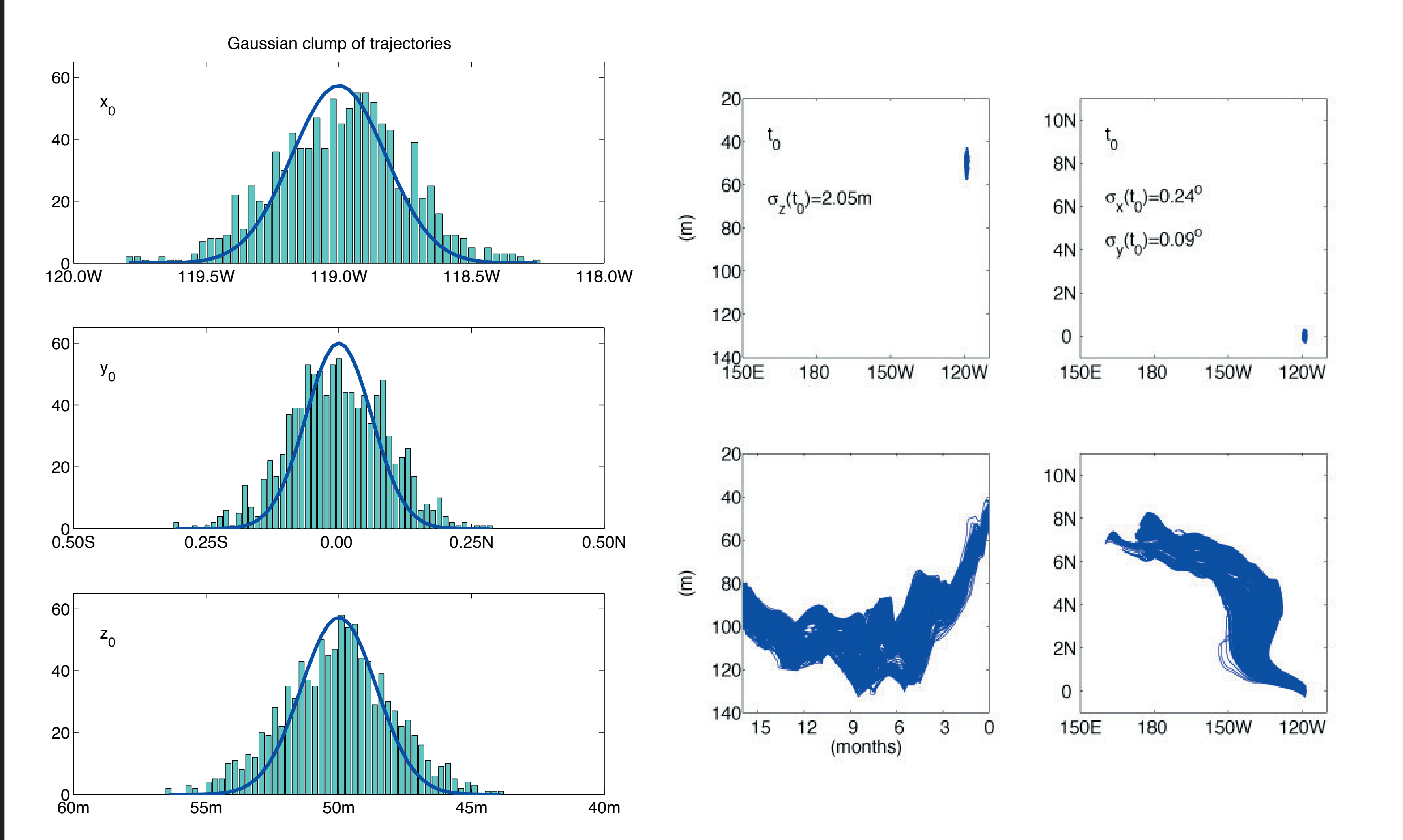
The pathways and diagnostic terms responsible for the eastern equatorial warm anomaly do not appear to sensitively depend on the particular mixed layer dynamics of the numerical model.



These same four model runs were used to evaluate whether the dynamics of the western Pacific off-equatorial cool anomalies are sensitive to model mixed layer dynamics, since upwelling was found to be so important in this region. The heat content anomalies are shown above for the 4 runs. The positions of the anomalies are slightly different, so different locations were used for the trajectories, as indicated by the white dots. The diagnostic terms accounting for these anomalies, though, are consistent between the runs. These are shown in bar graphs on the left, for 100m thick depth bins in each anomaly. The colors are the same as for the warm anomaly.

## Gaussian Clump of Trajectories

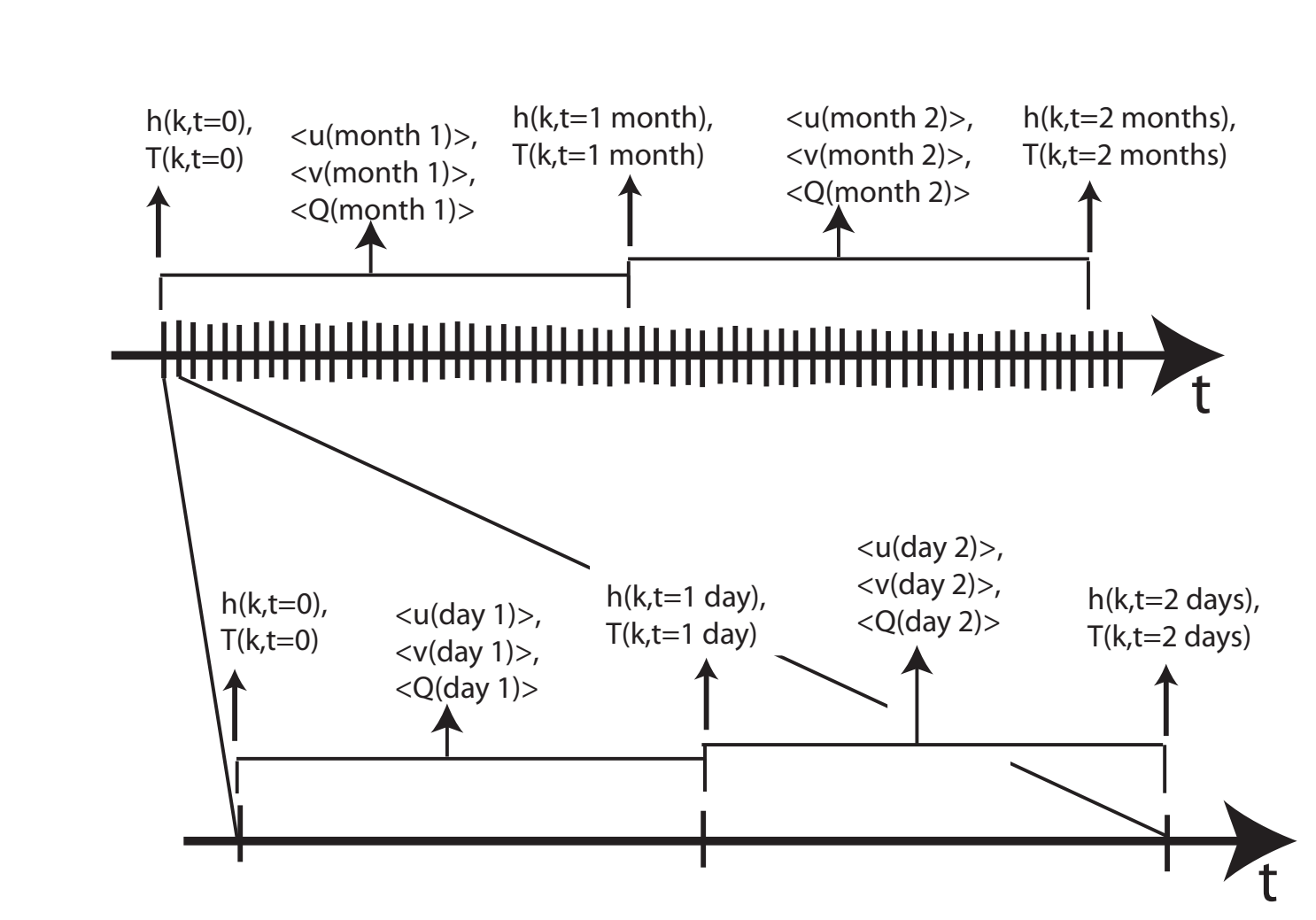
Another concern was that our method for computing trajectories backwards in time might be sensitive to the start position of the trajectory. To check this, we computed trajectories for a test set of 1000 start positions. These positions were chosen to be in a Gaussian distribution in x, y, and z about the point 119°W, the equator, and z=50m. These are all within the ENSO warm anomaly region of the eastern equatorial Pacific. The distributions of these starting positions are shown in the figure below and to the left. The top, middle, and bottom panels show the distribution in x, y, and z, respectively. Trajectories were then computed from these locations backwards 16 months from the month of the peak warm anomaly in our composite ENSO event. These trajectories are shown in the figure below and to the right. The top panels show the start positions again for reference, and the bottom panels show the 16 month trajectories. On the left, the positions and trajectories are plotted versus latitude on the x-axis and depth on the y-axis. On the right, they are plotted in horizontal map view. There is some spread to be seen as these trajectories go back in time. However, as the figure below (right) shows, these trajectories are consistent in character. These all follow the same basic pathway, the Northern Interior Pathway which is described in the sections above. Further, they all come from the same part of the water column, within 20m of one another in the vertical by the time they have travelled back 16 months.



## Daily vs. Monthly Model Output Fields

We are in the process of completing an additional check on the results of this study. All of the trajectories computed so far, discussed in the previous sections of this poster, were computed from monthly output of the model. The actual model time step is one hour. It is impractical, however, to output every time step of a multi-decadal model run. The model layer thicknesses, h, and the temperatures, T, are output as snapshots every month. The velocities, u and v, and the vertical heat flux, Q, are averaged over one month periods and output. The trajectories are then computed, generating daily positions for water parcels from these monthly model fields.

To determine the reliability of the above method, we are completing an additional model run, with h and T output as daily snapshots and u, v, and Q as daily averages. This is illustrated in the figure at right. This run will be just over one model year in length. We will then compute new trajectories using daily output fields of h, T, u, v, and Q, and compare these to the trajectories previously computed from the monthly fields.



## Summary

We have completed several checks of our results, shown at previous SWT meetings. There is still some to be done, specifically the daily vs. monthly model output check described above. The results so far, however, indicate that our results are not sensitive to the particular mixed layer dynamics of the numerical model, that our composite is a reasonable approximation of at least the 1997 warm event, and that random variations do not dominate the trajectory computation (based on the Gaussian trajectory clump described in the section at left).

We therefore have increased confidence in our results as previously stated. Among these are that the eastern equatorial warm anomaly is due primarily to variations in three major pathways into the region, and that the western Pacific off-equatorial cool anomalies are due to ENSO-related anomalous Ekman pumping.

## Acknowledgements

The work was supported by NASA and the Jet Propulsion Laboratory as part of the TOPEX Altimeter Research in Ocean Circulation and the JASON-1 project. C. Holland was partially supported by a NASA Earth System Science Fellowship. We thank R. Murtugudde, A. Busalacchi, R. Weisberg, M. Luther and F. Muller-Karger for many helpful discussions.